



Integrated Geochemical and Multivariate Assessment of Heavy Metal Contamination and Ecological Risk in Ikpoba and Ogba Rivers Benin City Edo State, Nigeria



Ozekeke Ogbeide^{1*} & Grace Ogbeide²

^{1,2}Department of Environmental management and Toxicology, Faculty of Life Sciences, University of Benin

*Corresponding Author Email: ozekeke.ogbeide@uniben.edu

ABSTRACT

Urbanization-driven contamination of freshwater systems has become an increasing environmental concern due to the persistence, bioaccumulation potential, and ecological toxicity of heavy metals in aquatic environments. This study presents an integrated geochemical and multivariate assessment of heavy metal contamination and ecological risk in the Ikpoba and Ogba Rivers located in Benin City, Edo State, Nigeria. Surface water and sediment samples were collected and analyzed for Pb, Cd, Mn, Fe, Cu, Zn, and Ni using atomic absorption spectrophotometry. To determine contamination levels and ecological implications, several geochemical indices including contamination factor (CF), geo-accumulation index (I_{geo}), enrichment factor (EF), and potential ecological risk index (PERI) were applied. In addition, multivariate statistical approaches such as Pearson correlation analysis, principal component analysis (PCA), and hierarchical cluster analysis were employed to identify relationships among metals and distinguish between lithogenic and anthropogenic sources. The results showed substantially higher concentrations of heavy metals in sediments compared with water, indicating strong sediment–water partitioning influenced by adsorption processes involving Fe–Mn oxides and particulate matter. The dominance of iron and manganese reflects natural lithogenic contributions associated with tropical lateritic geology, while strong associations among Cd, Zn, Ni, Pb, and Cu indicate common anthropogenic inputs from urban runoff, industrial discharge, and municipal waste pathways. Although contamination factors and geo-accumulation indices suggest generally low to moderate contamination, enrichment factors revealed notable anthropogenic enrichment of cadmium and copper. Cadmium was identified as the major ecological risk driver due to its high toxic-response coefficient. Overall, the study demonstrates that the Ikpoba and Ogba Rivers are experiencing early-stage anthropogenic metal enrichment moderated by sediment retention processes but remain vulnerable to future ecological risk under changing environmental conditions.

Keywords:

Heavy metals,
Tropical River systems,
Nigeria,
Urban watersheds,
Sediment contamination

INTRODUCTION

Freshwater ecosystems play a critical role in sustaining biodiversity, regulating biogeochemical cycles, and supporting human populations through water supply, fisheries, and agriculture (Adubor *et al.*, 2025; Anyanwu *et al.*, 2023). However, rapid urbanization, industrial expansion, and population growth have intensified contaminant loading into river systems, particularly in developing regions where wastewater infrastructure and environmental regulation remain limited (Bawa-Allah, 2023; Nkwunonwo *et al.*, 2020).

Among emerging environmental concerns, heavy metal pollution is of particular significance because of its persistence, non-biodegradability, and capacity for bioaccumulation across trophic levels (Adamu *et al.*, 2026; Ali *et al.*, 2019). Recent global assessments indicate that urban rivers increasingly function as integrative sinks for anthropogenic metals, reflecting complex interactions between natural geochemical processes and human-derived inputs (Gampson *et al.*, 2025; Tiabou *et al.*, 2024).

In tropical environments, intense chemical weathering and lateritic soil development strongly influence metal cycling. Iron and manganese oxides derived from weathered parent materials act as key sorptive phases controlling trace metal mobility through adsorption, co-precipitation, and redox-sensitive transformations (Ansart *et al.*, 2022; Swanson *et al.*, 2023). Consequently, sediments frequently contain the majority of the metal burden in aquatic systems, in some cases exceeding 90% of total loads (Imiuwa *et al.*, 2014; Okwodu *et al.*, 2021; Sadiq *et al.*, 2026). While sediment sequestration may reduce immediate dissolved-phase exposure, metals bound to sediments are not permanently immobilized. Changes in physicochemical conditions, including shifts in redox potential, organic matter decomposition, or hydrological disturbances, can destabilize metal–sediment associations (Ferrans *et al.*, 2021; Prabhakaran *et al.*, 2019). Under such conditions, previously sorbed metals may be remobilized into the water column, allowing sediments to function as secondary sources of contamination (Anyanwu *et al.*, 2023; Chris *et al.*, 2023; Maqsood and Lobos-Moysa, 2025).

Assessing contamination dynamics requires analytical approaches that go beyond measuring metal concentrations alone. Recent environmental studies increasingly combine standardized contamination indices, such as the geo-accumulation index (Igeo), contamination factor (CF), enrichment factor (EF), and potential ecological risk index (PERI), with multivariate statistical analyses to improve interpretation of pollution sources and ecological risk patterns (Abdu-Raheem *et al.*, 2024; Okafor *et al.*, 2024). These integrated approaches help distinguish natural lithogenic background contributions from anthropogenic enrichment, particularly in urbanized tropical watersheds where multiple pollution sources overlap and interact (Fadlillah *et al.*, 2023).

The Ikpoba and Ogba Rivers in Benin City represent important freshwater systems increasingly subjected to anthropogenic pressures including brewery effluents, urban stormwater discharge, vehicle maintenance activities, agricultural runoff, and municipal waste inputs (Adubor *et al.*, 2025; Ologbosere and Aluyi, 2016; Wangboje and Braimah, 2022). Previous investigations have reported elevated heavy metal concentrations in water, sediments, and aquatic organisms within these rivers (Ogbeide and Ogbeide, 2024). However, most existing studies have focused primarily on concentration-

based assessments, with limited attention to the underlying geochemical partitioning processes that regulate metal distribution between water and sediments. In particular, integrated evaluations that combine sediment–water partitioning dynamics with multivariate statistical techniques for source identification and ecological risk assessment remain scarce for these river systems.

This study therefore evaluates the environmental distribution, contamination status, and ecological risk of heavy metals in the Ikpoba and Ogba Rivers using an integrated geochemical and statistical framework. Specifically, contamination indices, multivariate statistical analyses, and sediment–water partitioning assessments were applied to distinguish lithogenic background contributions from anthropogenic enrichment and to provide a more comprehensive understanding of contamination dynamics within these urban tropical river systems.

MATERIALS AND METHODS

Study Area and Sampling

The study was conducted in Benin City, Edo State, within the western littoral hydrological area of Southern Nigeria (Ogbeide and Ogbeide, 2024). The investigation focused on two major 4th-order lotic systems: the Ikpoba River and the Ogba River, which are critical tributaries of the Ossiomo River (Ogbeide and Edene, 2023).

i. Ikpoba River

Positioned at latitudes 6°11' to 6°29'N and longitudes 5°33' to 5°47'E, this river originates from the Northern Ishan Plateau (Ogbeide and Ogbeide, 2024; Wangboje and Ekundayo, 2013). It traverses urban centers where it receives significant anthropogenic inputs from brewery effluents, municipal waste, and urban stormwater runoff (Adubor *et al.*, 2025; Ologbosere and Aluyi, 2016).

ii. Ogba River

Located at approximately latitude 6.20°N and longitude 5.34°E, the Ogba is a 42 km long perennial rainforest river (Anyanwu, 2012). It serves as the primary recipient for Benin City's master drainage system, which introduces mixed effluents from vehicle maintenance workshops, agricultural sites, and residential areas (Wangboje and Braimah, 2022).

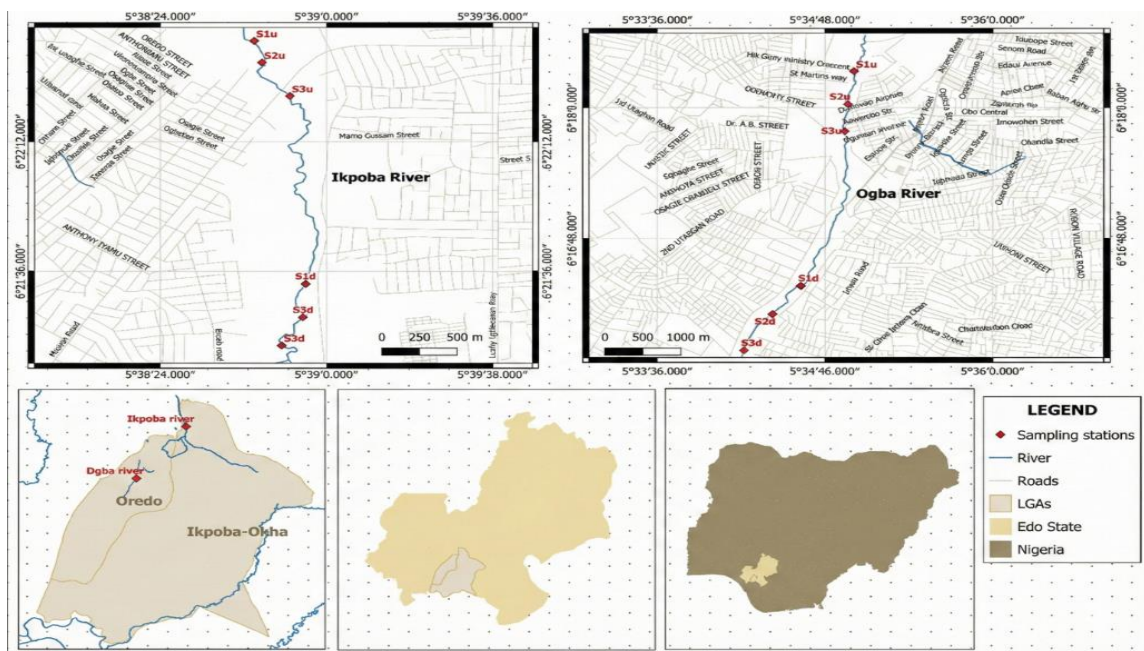


Figure 1: Map of the study area in Benin City showing the 4th-order lotic systems (Ikpoba and Ogba Rivers) and the sites selected for surface water and sediment sampling."

Sampling Protocol

Surface water samples were collected at a depth of approximately 30 cm using pre-cleaned polyethylene bottles (Wangboje and Braimah, 2022; Wangboje and Ekundayo, 2013). To stabilize metal ions and prevent wall adsorption, samples were acidified in-situ with concentrated analytical-grade nitric acid (HNO_3) to a $\text{pH} < 2$ (Odo *et al.*, 2024; Shinkafi *et al.*, 2023). Bottom sediment samples were retrieved using an Ekman or Van Veen grab sampler (Imiuwa *et al.*, 2014; Ogbeide and Ogbeide, 2024). Composite samples were formed at each station to ensure representativeness, placed in labeled acid-cleaned containers, and transported to the laboratory in ice chests maintained below 4°C (Ogbeide and Okoduwa, 2024; Wangboje and Ekundayo, 2013).

Chemical Analysis

Water and sediment samples were analyzed for heavy metals, including Cd, Cr, Mn, Ni, Pb, Fe, Cu, and Zn. For water samples, 100 mL aliquots were filtered ($0.45 \mu\text{m}$) and acid-digested (Shinkafi *et al.*, 2023). Sediment samples were oven-dried at 60°C to a constant weight, pulverized, and sieved through a 2 mm mesh screen (Adubor *et al.*, 2025; Wangboje and Ekundayo, 2013). Digestion was performed using Aqua-Regia (HNO_3 -HCl mixture) or concentrated HNO_3 on a hot plate (Eyenubo *et al.*, 2023)

Metal concentrations were quantified using Flame Atomic Absorption Spectrophotometry (AAS), utilizing the Buck Scientific 210VGP. Quality assurance was maintained through the use of reagent blanks, triplicate analysis of samples, and comparison with certified

standard reference materials (SRMs) to ensure accuracy and precision (Abdu-Raheem *et al.*, 2024; Shinkafi *et al.*, 2023).

Quality Assurance and Quality Control

To ensure the reliability and accuracy of analytical results, a comprehensive quality assurance and quality control (QA/QC) protocol was implemented throughout the study. All sampling and laboratory containers were thoroughly pre-cleaned using 10% analytical-grade nitric acid (HNO_3) and subsequently rinsed with deionized water to minimize contamination.

Quality control procedures included the use of procedural blanks, certified standard reference materials (SRMs), and replicate analyses. Procedural blanks were processed alongside each batch of samples to detect any potential contamination introduced during sample preparation or analysis. The accuracy of the analytical method was verified using certified standard reference materials, with recovery rates for all analyzed metals ranging between 92% and 106%, indicating acceptable analytical accuracy.

Analytical precision was evaluated through triplicate analysis of each sample, and the relative standard deviation (RSD) for replicate measurements was maintained below 10%. Instrument calibration was carried out using multi-element standard solutions prepared from analytical-grade stock standards. Calibration curves exhibited excellent linearity with coefficients of determination (R^2) greater than 0.999 for all metals analyzed.

Sediment Contamination Indices

Sediment contamination levels were evaluated using widely applied geochemical indices, including the Contamination Factor (CF), Pollution Load Index (PLI), Geo-accumulation Index (I_{geo}), and Enrichment Factor (EF). These indices provide quantitative measures of contamination intensity, anthropogenic enrichment, and overall pollution status of sediments.

i. **Contamination Factor (CF)**

The contamination factor represents the ratio of the measured concentration of a metal in sediment to its corresponding geochemical background value (Hakanson, 1980). Background values were adopted from Average Shale Values or local uncontaminated reference levels (Abdu-Raheem *et al.*, 2024).

$$CF_i = \frac{C_i}{B_i} \tag{1}$$

where C_i is the measured concentration of metal i in the sediment sample and B_i is the background concentration of the same metal.

ii. **Pollution Load Index (PLI)**

The pollution load index provides an integrated assessment of the overall level of heavy metal pollution at each sampling location. It is calculated as the n th root of the product of individual contamination factors (Tomlinson *et al.*, 1980).

$$PLI = (CF_1 \times CF_2 \times CF_3 \times \dots \times CF_n)^{\frac{1}{n}} \tag{2}$$

where n represents the number of metals analyzed.

iii. **Geo-accumulation Index (I_{geo})**

The geo-accumulation index evaluates the degree of metal contamination in sediments by comparing present concentrations with pre-industrial background levels while accounting for natural lithogenic variability (Muller, 1969).

$$I_{geo} = \log_2 \left(\frac{C_n}{1.5 \times B_n} \right) \tag{3}$$

where C_n represents the measured concentration of the metal in the sediment, B_n is the background value, and the factor **1.5** accounts for natural variations in lithogenic metal concentrations.

v. **Enrichment Factor (EF)**

The enrichment factor is used to distinguish anthropogenic metal inputs from natural geogenic sources by normalizing metal concentrations against a conservative reference element, commonly iron (Fe) (Ayedun, 2021; Tiabou *et al.*, 2024).

$$a. \quad EF = \frac{\left(\frac{C_i}{C_{ref}} \right)_{sample}}{\left(\frac{B_i}{B_{ref}} \right)_{background}} \tag{4}$$

where C_i and B_i represent the concentration and background value of metal i , while C_{ref} and B_{ref} denote the concentration and background value of the reference element (Fe).

Potential Ecological Risk Assessment

The Potential Ecological Risk Index (PERI) was applied to assess the overall ecological risk posed by heavy metal contamination in the aquatic environment following the method proposed by Hakanson (1980). The ecological risk factor for each metal E_r^i was calculated as

$$E_r^i = T_r^i \times CF_i \tag{5}$$

where T_r^i represents the toxic-response factor for metal i , and CF_i is the contamination factor. Toxic-response factors adopted were Cd (30), Pb (5), Cu (5), Ni (5), Cr (2), and Zn (1), consistent with established literature (Hakanson, 1980; Ogbeide and Ogbeide, 2024).

The comprehensive risk index (RI) was the summation of all individual risk factors (Hakanson, 1980; Tiabou *et al.*, 2024).

$$RI = \sum_{i=1}^n E_r^i \tag{6}$$

where n is the total number of metals analyzed.

Statistical and Multivariate Analysis

Data were processed using SPSS (versions 22) and Microsoft Excel (Ogbeide and Okoduwa, 2024; Sani *et al.*, 2022). Descriptive statistics (mean, standard deviation, coefficient of variation) were used to characterize metal distribution. Before inferential testing, data were subjected to normality testing using the Shapiro-Wilk framework (Adubor *et al.*, 2025). One-way ANOVA and Duncan Multiple Range (DMR) tests were used to evaluate significant differences between sampling locations at $p < 0.05$ (Ogbeide and Okoduwa, 2024; Sani *et al.*, 2022).

Multivariate statistical techniques were employed for source apportionment of heavy metals. Pearson's correlation coefficients were computed to establish inter-element associations and infer possible common origins (Sani *et al.*, 2022). Principal Component Analysis (PCA), with Varimax rotation, was applied to extract dominant factors and identify potential pollution sources based on factor loadings and eigenvalues (Abdu-Raheem *et al.*, 2024; Eyenubo *et al.*, 2023). In addition, Hierarchical Cluster Analysis (HCA) was conducted to classify sampling sites or elements into homogeneous groups according to similarities in their pollution profiles,

thereby supporting interpretation of spatial patterns and source contributions (Abdu-Raheem *et al.*, 2024).

RESULTS AND DISCUSSION

Heavy metals were detected in both the aqueous and sediment matrices, although their concentration ranges and variability patterns differed markedly between the two environmental compartments. Descriptive statistics summarizing central tendency and dispersion for metals in surface water are presented in Table 1, while corresponding distributional characteristics for sediment-associated metals are provided in Table 2. Temporal patterns in metal concentrations within the aqueous phase across sampling months and between river systems are illustrated in Figure 2, whereas temporal trends for sediment-associated metals are presented in Figure 3. Comparative distribution patterns between the two matrices are shown in Figure 4, highlighting differences in metal accumulation between water and sediments. Variability and dispersion characteristics within the datasets are further illustrated using box-and-whisker plots in Figures 5a and 5b.

The distribution patterns observed in Tables 1 and 2 together with the graphical representations in Figures 2–5 reveal a clear geochemical compartmentalization between aqueous and sediment phases. Iron and manganese dominate both matrices, with markedly higher absolute concentrations recorded in sediments (Table 2; Figure 4). This pattern suggests strong lithogenic control typical of highly weathered tropical basins. Lateritic soils prevalent in humid tropical environments are naturally enriched in Fe- and Mn-oxides, which function as major sorbents for trace metals (Ansart *et al.*, 2022; Elarabi *et al.*, 2013; Qin *et al.*, 2018). Similar dominance of Fe and Mn in West African freshwater sediments has been reported by Bawa-Allah (2023) and Tiabou *et al.* (2024), who attributed elevated concentrations to oxidative precipitation and secondary mineral formation processes. The high Fe concentrations observed in sediments (Table 2) together with the sediment–water partition ratios (Table 10) further support the strong scavenging capacity of Fe-oxide phases in tropical aquatic systems.

Despite the dominant lithogenic influence, variability in certain trace metals indicates additional anthropogenic inputs. The high coefficients of variation recorded for Cd (137.6%) and Pb (39.4%) in water (Table 1; Figure 5a) suggest episodic rather than uniform geogenic supply. Urban runoff pulses and drainage discharges are known to generate transient spikes in dissolved metals, particularly in rapidly urbanizing tropical watersheds (Gampson *et al.*, 2025; Okafor *et al.*, 2024). Similar pulse-driven variability has been documented in Indonesian and West African urban rivers, where Cd and Pb concentrations exhibited strong temporal heterogeneity linked to rainfall-driven runoff events

(Ekoa Bessa, 2023; Fadlillah *et al.*, 2023). These observations therefore support a dual-source model in which a relatively stable lithogenic background is superimposed with periodic anthropogenic inputs.

Further insight into metal distribution is provided by the pronounced enrichment of metals in sediments relative to water (Figure 4; Table 10). This pattern confirms rapid adsorption and settling of metals onto particulate phases. Previous studies have shown that more than 90% of metals such as Cu, Pb, and Zn in fluvial systems occur in particle-bound forms due to strong affinities for Fe-oxhydroxides and organic matter (Ali *et al.*, 2019). Comparable sediment-dominated partitioning has been reported for the Ikpoba River (Adubor *et al.*, 2025) and for Cameroon's Limbe River (Tiabou *et al.*, 2024). The sediment enrichment observed in the present study therefore reflects adsorption equilibria, coagulation with suspended particulates, and gravitational settling processes.

In contrast, some highly urbanized watersheds in North America exhibit sustained dissolved-phase dominance due to complexation with dissolved organic carbon (Gampson *et al.*, 2025). The absence of such dominance in the present system suggests relatively lower dissolved organic carbon-driven complexation or rapid flocculation processes under tropical hydrochemical conditions.

To further elucidate relationships among metals, patterns of co-occurrence and inter-element associations were examined using correlation analysis. Numerical correlation coefficients for metals in the water matrix are summarized in Table 3, while the graphical representation of correlation strength and direction is provided in Figure 6.

Relationships among metals were first examined using correlation analysis to identify possible shared sources and geochemical associations. Strong positive correlations among Pb, Cd, Zn, Ni, and Cu in water (Table 3; Figure 6) indicate common transport pathways or co-emission sources. Similar clustering patterns have been reported in southwestern Nigeria by Abdu-Raheem *et al.* (2024), who associated these metals with industrial discharge and urban runoff. Comparable Pb–Cu–Zn groupings were also documented in Indonesian urban rivers, where vehicular emissions and metallurgical activities were identified as major contributors (Fadlillah *et al.*, 2023). The consistency between these previous findings and the correlation structure observed in Table 3 supports the interpretation of anthropogenic co-loading within the studied river systems.

In contrast, Mn and Fe display weaker correlations with the other trace metals (Table 3), suggesting that their distribution is primarily controlled by lithogenic sources rather than direct anthropogenic inputs. A similar separation between Fe–Mn and anthropogenic trace metals was reported by Tiabou *et al.* (2024), who observed that Fe and Mn largely reflected crustal

background contributions while Cd and Pb were associated with urban contamination. However, the apparent independence of Fe and Mn in correlation analysis does not imply that they are environmentally isolated from trace metal dynamics. Iron and manganese oxides play a fundamental role in regulating trace metal mobility through redox-controlled adsorption and dissolution processes (Swanson *et al.*, 2023). Under reducing conditions, dissolution of Fe–Mn oxyhydroxides can release sorbed metals such as Cd and Pb into pore water, increasing their bioavailability and ecological risk (Ali *et al.*, 2019; Chris and Anyanwu, 2023). Consequently, although Fe and Mn appear geochemically distinct based on correlation patterns, they remain functionally linked to trace metal behavior through sediment redox cycling.

Correlation analysis of sediment-associated metals (Table 4; Figure 7) reveals a Cu–Zn–Ni grouping that is consistent with co-adsorption onto fine-grained sediment particles. Similar patterns were documented by Eyenubo *et al.* (2023), who attributed Cu–Zn clustering in dredged tributaries to industrial effluent inputs. Conversely, the relatively weak Pb–Cu relationship observed in the present sediments differs from patterns reported in highly industrialized estuaries where stronger Pb–Cu associations occur (Gampson *et al.*, 2025). This difference suggests that although anthropogenic inputs are present in the studied rivers, the intensity of industrial contamination may be moderate rather than severe.

To further evaluate contamination status and ecological implications, several sediment contamination indices were calculated. Contamination factors, enrichment factors, geo-accumulation indices, and ecological risk factors are summarized in Table 5 and illustrated in Figure 8. The results indicate that sediment contamination levels across the Ikpoba and Ogba Rivers generally fall within low to moderate categories. This observation is consistent with recent assessments of Nigerian freshwater systems, where anthropogenic signatures are detectable but absolute concentrations frequently remain below severe toxicity thresholds (Abdu-Raheem *et al.*, 2024; Okafor *et al.*, 2024). Similar moderate contamination levels were reported for Ikpoba River sediments by Adubor *et al.* (2025), who concluded that the system is impacted by urban pressures but has not yet reached advanced ecological degradation.

Despite the moderate contamination levels indicated by CF and Igeo values, enrichment factor results provide additional insight into anthropogenic metal contributions. Elevated EF values for cadmium and copper indicate enrichment beyond natural lithogenic weathering processes (Abdu-Raheem *et al.*, 2024; Fadlillah *et al.*, 2023). This enrichment reflects the role of sediments as long-term repositories for trace metals, where adsorption and co-precipitation with Fe–Mn oxides facilitate metal accumulation (Chris and Anyanwu, 2023; Mekuria *et al.*,

2020). The elevated enrichment of Cd and Cu aligns with observations from Niger Delta and Indonesian urban rivers, where these metals were strongly associated with municipal effluents, mechanic workshops, and agricultural runoff (Chris and Anyanwu, 2023; Fadlillah *et al.*, 2023).

Cadmium emerged as the dominant ecological risk contributor within the studied systems (Table 5). This dominance is largely explained by its exceptionally high toxic-response coefficient ($Tr = 30$), which amplifies its ecological impact relative to other metals such as Pb or Zn (Hakanson, 1980; Ogbeide and Ogbeide, 2024). Similar findings have been reported in regional meta-analyses of Nigerian freshwater environments, where Cd consistently appears as the principal driver of ecological risk (Bawa-Allah, 2023). Comparable Cd-driven ecological threats have also been documented in the Limbe River in Cameroon and the Osse River in Nigeria, suggesting a broader regional pattern of urban contamination in tropical river systems (Tiabou *et al.*, 2024; Uwaifo *et al.*, 2023).

Although the cumulative potential ecological risk index (RI) remains below high-risk thresholds (Table 5; Figure 8), this classification should not be interpreted as evidence of negligible ecological impact. Previous studies have shown that chronic exposure to mixtures of trace metals, even at moderate concentrations, can induce oxidative stress and impair physiological processes in aquatic organisms (Ali *et al.*, 2019; Shinkafi *et al.*, 2023). The results therefore suggest that the Ikpoba and Ogba Rivers are currently in a transitional contamination stage characterized by early cumulative stress. Continuous monitoring and proactive management are necessary to prevent progression toward the higher risk levels observed in more industrialized basins (Ibezute *et al.*, 2016; Okafor *et al.*, 2024).

Multivariate statistical techniques were further applied to distinguish geogenic and anthropogenic influences on metal distribution. Principal Component Analysis was performed separately for water and sediment datasets, with eigenvalues and variance contributions summarized in Table 6 and illustrated in Figure 9. Component loading scores for water-associated metals are presented in Table 7 and visualized in Figure 10, while eigenvalue structures and loading patterns for sediment metals are provided in Tables 8 and 9 and illustrated in Figures 11 and 12. These multivariate approaches are widely applied in environmental geochemistry because they allow identification of dominant pollution sources within complex urban river systems where multiple contamination pathways overlap (Abdu-Raheem *et al.*, 2024; Sani *et al.*, 2022).

Within the water dataset, the first principal component explained 48.05% of total variance and exhibited strong loadings for Pb, Cu, Zn, and Ni (Table 6; Table 7; Figure 10). This pattern suggests a dominant anthropogenic

factor associated with urban-industrial activities. Similar PC1 configurations have been documented in West African urban rivers where trace metal assemblages were linked to municipal drainage and industrial effluents (Abdu-Raheem *et al.*, 2024; Adeleke *et al.*, 2022; Tiabou *et al.*, 2024). In contrast, studies conducted in less industrialized watersheds have reported lithogenic elements such as Fe and Al as the primary variance drivers (Fadlillah *et al.*, 2023), indicating that anthropogenic influence in the present rivers is comparatively stronger.

The sediment PCA results reveal a more distributed loading structure reflecting the integrative nature of sediment deposition and post-depositional transformation. One component characterized by strong Fe loading indicates persistent lithogenic influence consistent with mineral weathering inputs (Ekoa Bessa, 2023; Tiabou *et al.*, 2024). However, the presence of anthropogenic trace metal clusters within other components confirms that sediment contamination reflects a combination of natural geological inputs and ongoing human activities.

This dual structure has important implications for long-term environmental behavior. While lithogenic Fe–Mn phases contribute to baseline metal distribution, they also regulate trace metal mobility through redox cycling. Under reducing conditions, dissolution of Fe–Mn oxides can release previously adsorbed anthropogenic metals, transforming sediments from contaminant sinks into secondary sources (Abdu-Raheem *et al.*, 2024; Lynch *et al.*, 2014; Swanson *et al.*, 2023). Consequently, the PCA-

derived separation between geogenic and anthropogenic components reflects interacting processes rather than complete environmental independence.

Further insight into metal behavior was obtained from sediment–water partitioning analysis. Mean-based partition ratios (Table 10) and the graphical representation in Figure 13 indicate strong preferential accumulation of metals within sediment phases. Such high sediment–water partition ratios confirm that particulate adsorption processes dominate metal distribution in the studied rivers. Similar sediment-dominated partitioning has been reported in Ikpoba River (Adubor *et al.*, 2025) and in Orashi River sediments (Okwodu *et al.*, 2021), reflecting strong affinity of metals such as Cu, Pb, and Zn for organic matter and iron oxide surfaces (Ali *et al.*, 2019).

Nevertheless, sediment sequestration does not imply permanent immobilization. Previous studies have shown that under reducing conditions the dissolution of Fe–Mn oxides can release previously bound metals, allowing sediments to function as secondary contamination sources (Anyanwu *et al.*, 2023). Seasonal redox fluctuations typical of tropical river systems can therefore influence the remobilization of sediment-bound metals (Bawa-Allah, 2023). The sediment-dominated distribution observed in the present study should thus be interpreted as conditional sequestration dependent on environmental stability rather than permanent immobilization.

Table 1. Mean (\pm SD) concentrations of heavy metals in surface water samples from the study rivers.

| Metal | Concentration (mg/L) Mean \pm SD | Min | Max |
|-------|---------------------------------------|--------|-------|
| Pb | 0.0178 \pm 0.0070 | 0.0000 | 0.037 |
| Cd | 0.0028 \pm 0.0038 | 0.0000 | 0.009 |
| Mn | 0.0510 \pm 0.0087 | 0.033 | 0.066 |
| Fe | 0.3567 \pm 0.1138 | 0.0417 | 0.497 |
| Cu | 0.0972 \pm 0.0263 | 0.048 | 0.157 |
| Zn | 0.1415 \pm 0.0525 | 0.062 | 0.243 |
| Ni | 0.0492 \pm 0.0162 | 0.019 | 0.074 |

Table 2. Mean (\pm SD) concentrations of heavy metals in sediment samples from the study rivers.

| Metal | Concentration (mg/kg) Mean \pm SD | Min | Max |
|-------|--|--------|--------|
| Pb | 0.551 \pm 0.151 | 0.254 | 0.887 |
| Cd | 0.067 \pm 0.015 | 0.029 | 0.089 |
| Mn | 13.716 \pm 3.252 | 6.786 | 19.113 |
| Fe | 537.399 \pm 84.247 | 325.27 | 685.17 |
| Cu | 51.393 \pm 13.043 | 31.641 | 74.198 |
| Zn | 77.333 \pm 14.781 | 47.486 | 97.098 |

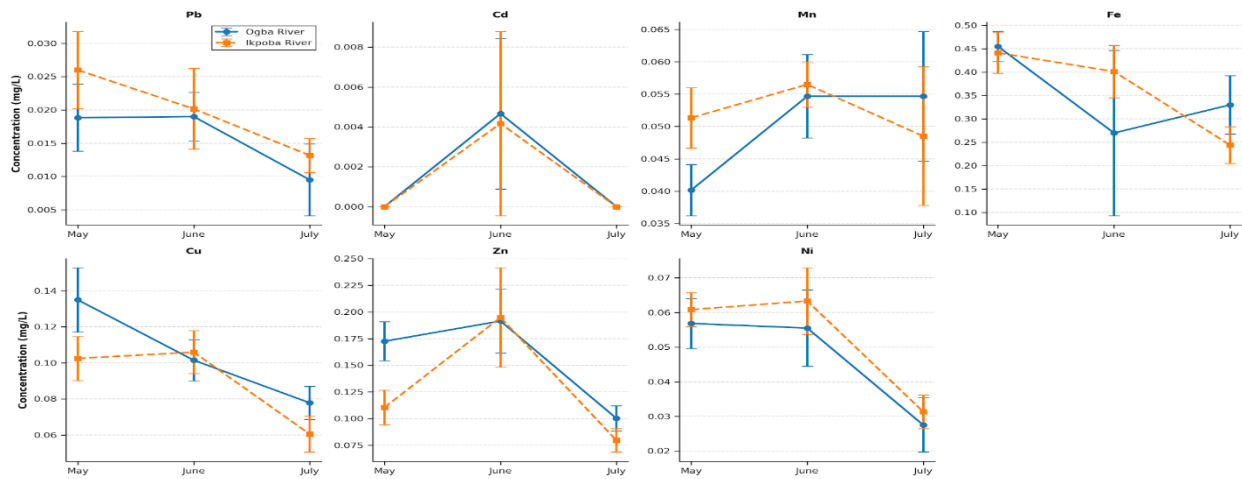


Figure 2: Temporal variation of heavy metal concentrations in water samples showing seasonal or sampling-period fluctuations and relative concentration trends.

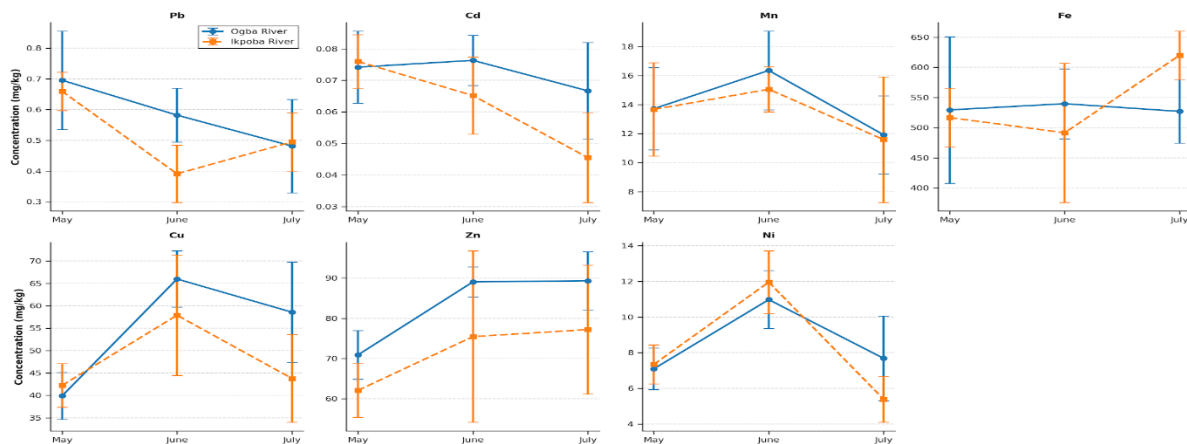


Figure 3: Temporal variation of heavy metal concentrations in sediment samples illustrating accumulation dynamics over the sampling period.

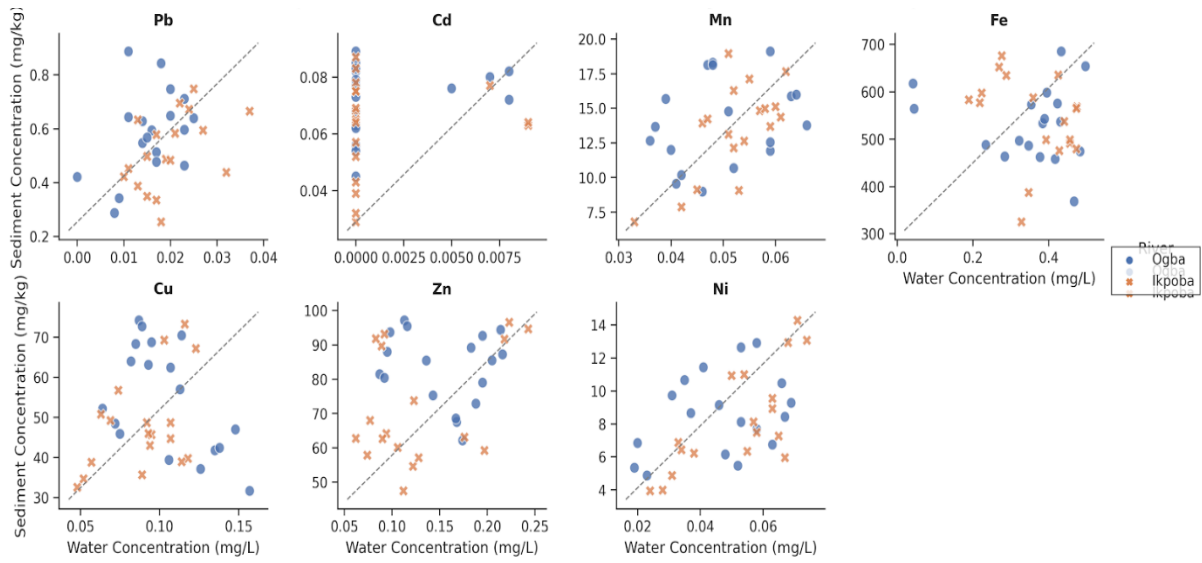


Figure 4: Comparative distribution of heavy metals between water and sediment matrices highlighting partitioning behaviour and accumulation differences.

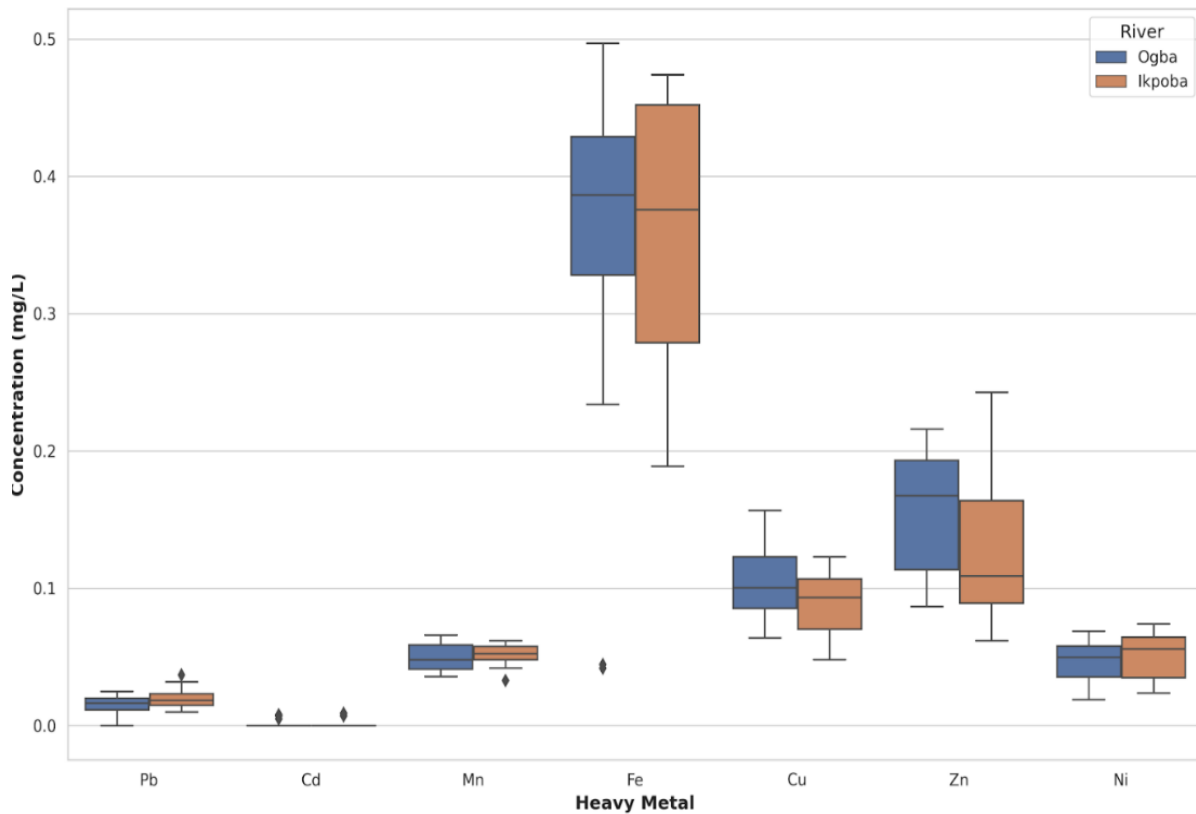


Figure 5a: Box-and-whisker plots showing variability and dispersion of heavy metal concentrations in water samples.

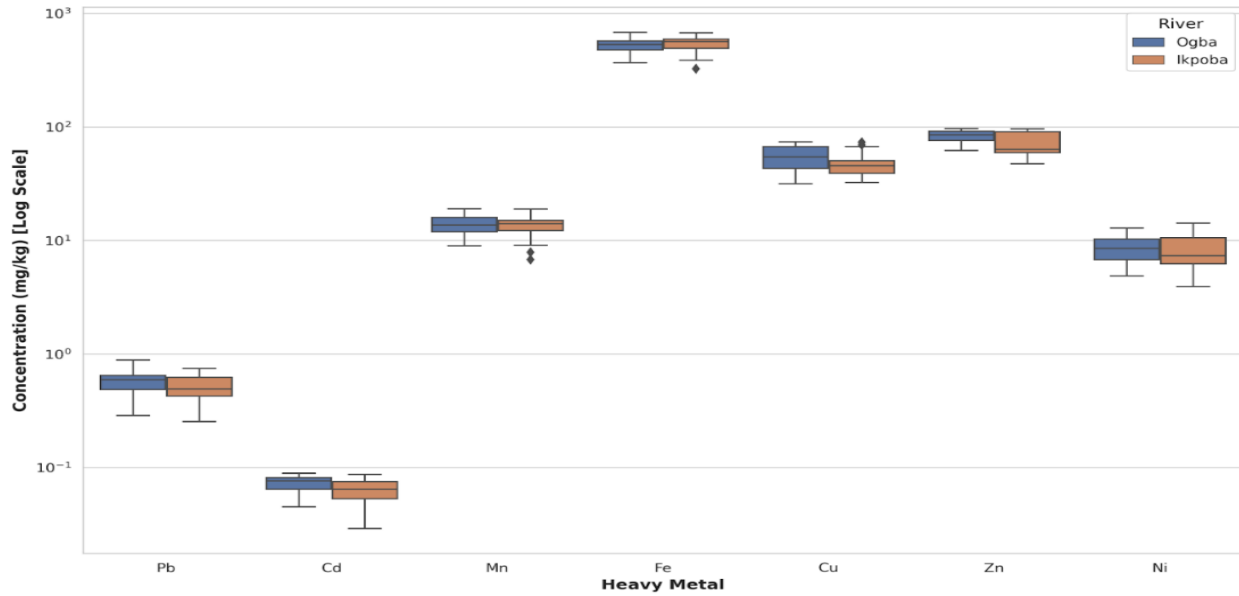


Figure 5b: Box-and-whisker plots showing variability and dispersion of heavy metal concentrations in sediment samples.

Table 3: Pearson correlation matrix for heavy metals in water samples showing inter-element relationships and potential shared sources or geochemical behaviour.

| | Pb | Cd | Mn | Fe | Cu | Zn | Ni |
|-----------|-----------|-----------|-----------|-----------|-----------|-----------|-----------|
| Pb | 1.000 | 0.780 | 0.238 | 0.350 | 0.415 | 0.416 | 0.792 |
| Cd | 0.780 | 1.000 | 0.370 | 0.144 | 0.861 | 0.968 | 0.941 |
| Mn | 0.238 | 0.370 | 1.000 | -0.112 | -0.169 | 0.203 | 0.173 |
| Fe | 0.350 | 0.144 | -0.112 | 1.000 | 0.509 | 0.201 | 0.434 |
| Cu | 0.415 | 0.861 | -0.169 | 0.509 | 1.000 | 0.589 | 0.660 |
| Zn | 0.416 | 0.968 | 0.203 | 0.201 | 0.589 | 1.000 | 0.703 |
| Ni | 0.792 | 0.941 | 0.173 | 0.434 | 0.660 | 0.703 | 1.000 |

Pearson Correlation Matrix (Water Samples)

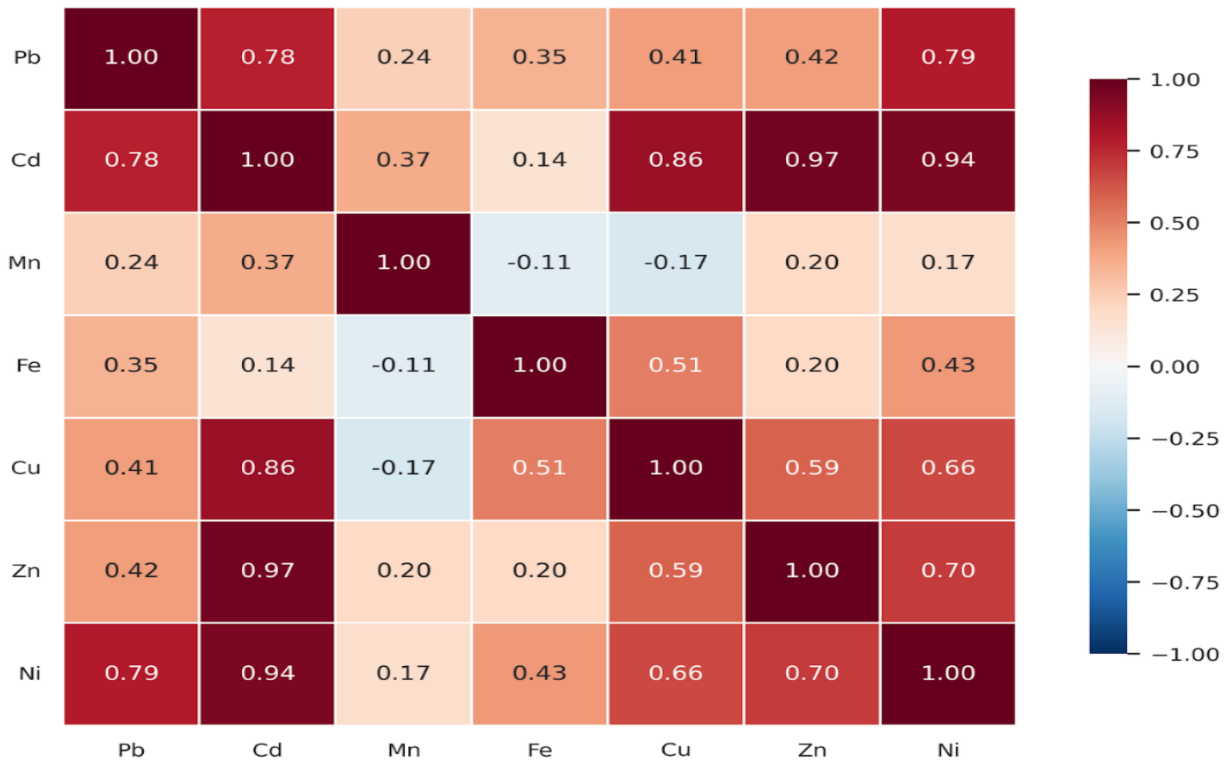


Figure 6: Correlation heatmap of heavy metals in water samples illustrating strength and direction of inter-element relationships.

Table 4: Pearson correlation matrix for heavy metals in sediment samples highlighting geochemical associations and co-occurrence patterns.

| | Pb | Cd | Mn | Fe | Cu | Zn | Ni |
|----|-----------|-----------|-----------|-----------|-----------|-----------|-----------|
| Pb | 1.000 | 0.637 | 0.187 | 0.345 | -0.052 | 0.020 | -0.077 |
| Cd | 0.637 | 1.000 | 0.450 | -0.058 | 0.312 | 0.185 | 0.367 |
| Mn | 0.187 | 0.450 | 1.000 | -0.077 | 0.419 | 0.284 | 0.674 |
| Fe | 0.345 | -0.058 | -0.077 | 1.000 | 0.170 | 0.351 | -0.154 |
| Cu | -0.052 | 0.312 | 0.419 | 0.170 | 1.000 | 0.792 | 0.740 |
| Zn | 0.020 | 0.185 | 0.284 | 0.351 | 0.792 | 1.000 | 0.397 |
| Ni | -0.077 | 0.367 | 0.674 | -0.154 | 0.740 | 0.397 | 1.000 |

Pearson Correlation Matrix (Sediment Samples)

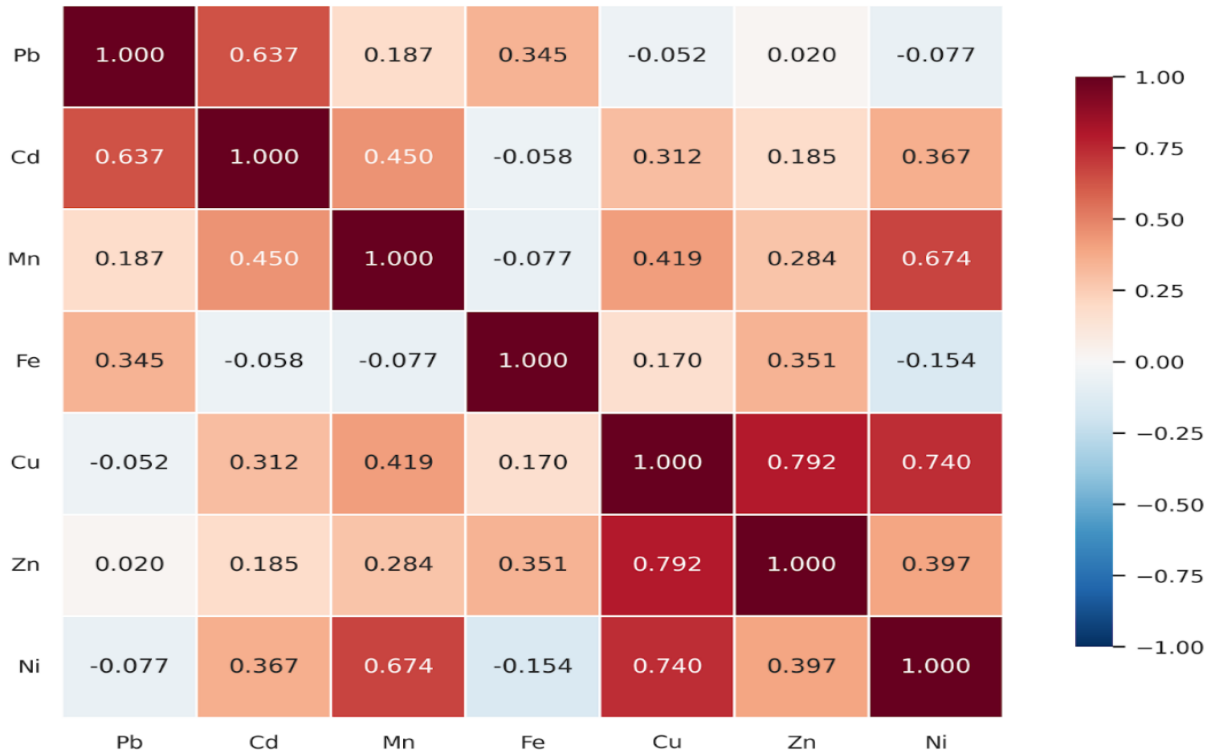


Figure 7: Correlation heatmap of heavy metals in sediment samples showing geochemical associations and possible shared sources.

Table 5. Sediment contamination indices for heavy metals indicating contamination status, anthropogenic enrichment, and ecological risk.

| Metal | Mean concentration (mg/kg) | Background (Bn) | CF | EF (Fe-normalized) | Igeo | Toxic response (Tr) | Ecological risk factor (Er = Tr × CF) |
|-------|----------------------------|-----------------|-------|--------------------|-------|---------------------|---------------------------------------|
| Pb | 0.551 | 20 | 0.028 | 2.42 | -5.77 | 5 | 0.138 |
| Cd | 0.067 | 0.30 | 0.224 | 19.72 | -2.74 | 30 | 6.731 |
| Mn | 13.716 | 850 | 0.016 | 1.42 | -6.54 | 1 | 0.016 |
| Fe* | 537.399 | 47,200 | 0.011 | — | -7.04 | — | — |
| Cu | 51.393 | 45 | 1.142 | 100.31 | -0.39 | 5 | 5.710 |
| Zn | 77.333 | 95 | 0.813 | 71.47 | -0.88 | 1 | 0.813 |
| Ni | 8.407 | 68 | 0.124 | 10.85 | -3.60 | 5 | 0.618 |

Note: *Fe was used as the reference element for enrichment factor normalization.

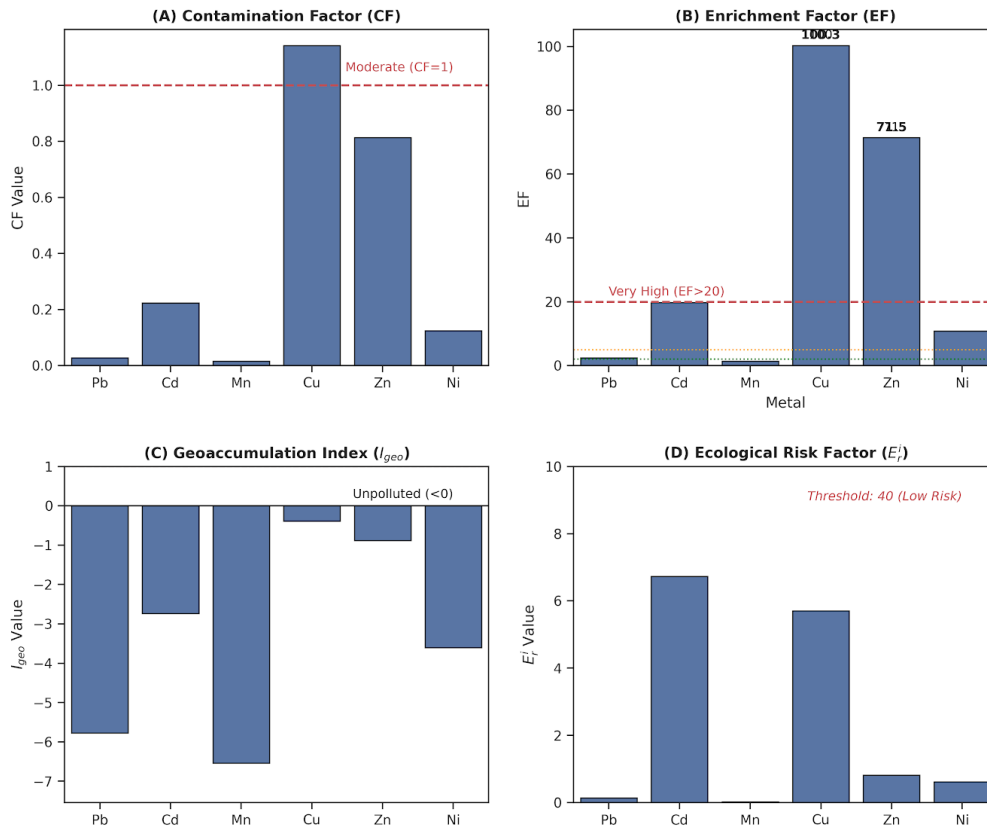


Figure 8: Ecological risk assessment outcomes for sediment heavy metals based on contamination indices and toxic response factors.

Table 6: Principal Component Analysis (PCA) eigenvalues and percentage variance explained for heavy metals in water samples used for source identification and dimensionality reduction.

| PC | Eigenvalue | Variance Explained (%) |
|-----|------------|------------------------|
| PC1 | 3.450 | 48.05 |
| PC2 | 1.647 | 22.87 |
| PC3 | 0.905 | 12.57 |
| PC4 | 0.556 | 7.72 |
| PC5 | 0.286 | 3.98 |
| PC6 | 0.232 | 3.23 |
| PC7 | 0.114 | 1.58 |

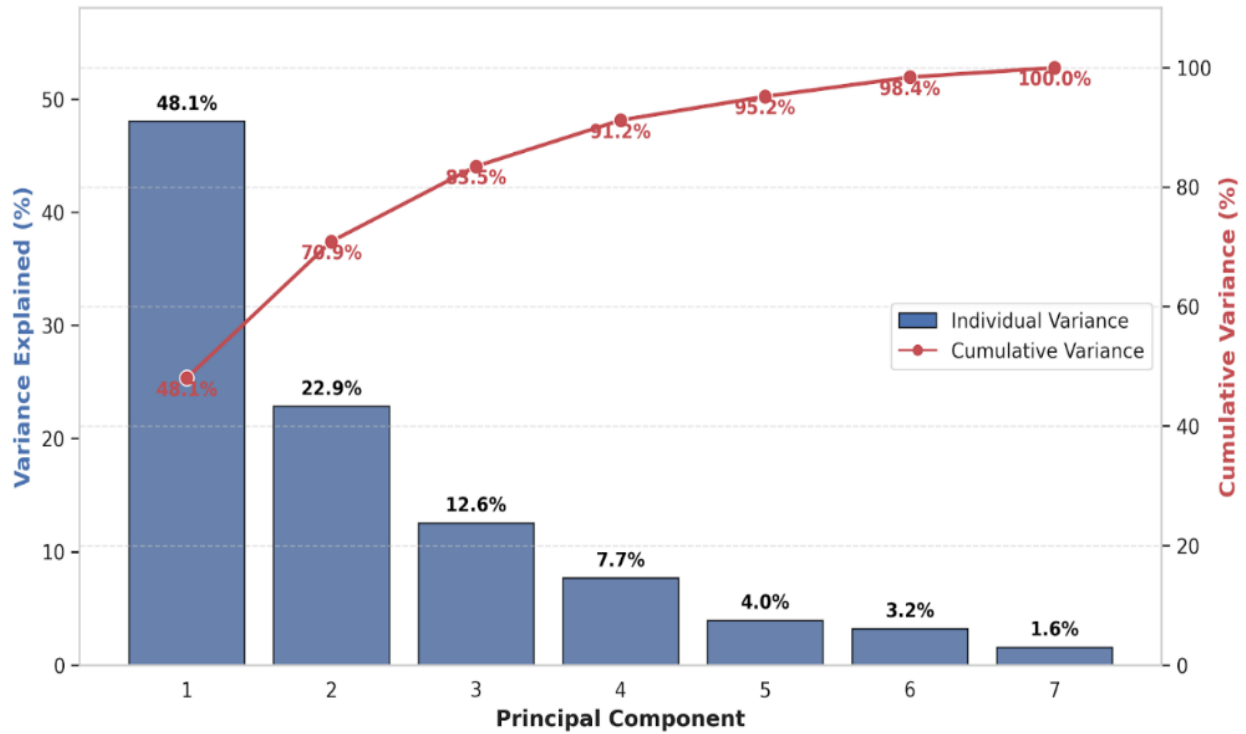


Figure 9: Scree plot showing variance explained by principal components for the water dataset.

Table 7: PCA loading scores showing contributions of individual heavy metals to principal components in the water dataset, indicating potential source grouping.

| Metal | PC1 | PC2 | PC3 | PC4 | PC5 | PC6 | PC7 |
|-------|-------|--------|--------|--------|--------|--------|--------|
| Pb | 0.417 | -0.030 | 0.467 | 0.600 | -0.034 | -0.050 | -0.494 |
| Cd | 0.332 | 0.505 | -0.323 | -0.047 | -0.418 | -0.595 | -0.024 |
| Mn | 0.136 | 0.566 | 0.556 | -0.457 | 0.377 | 0.026 | 0.023 |
| Fe | 0.253 | -0.532 | 0.342 | -0.555 | -0.455 | -0.129 | -0.062 |
| Cu | 0.408 | -0.337 | -0.316 | -0.148 | 0.679 | -0.347 | -0.125 |
| Zn | 0.453 | 0.152 | -0.377 | -0.206 | -0.116 | 0.697 | -0.296 |
| Ni | 0.511 | -0.056 | 0.099 | 0.238 | -0.016 | 0.143 | 0.805 |

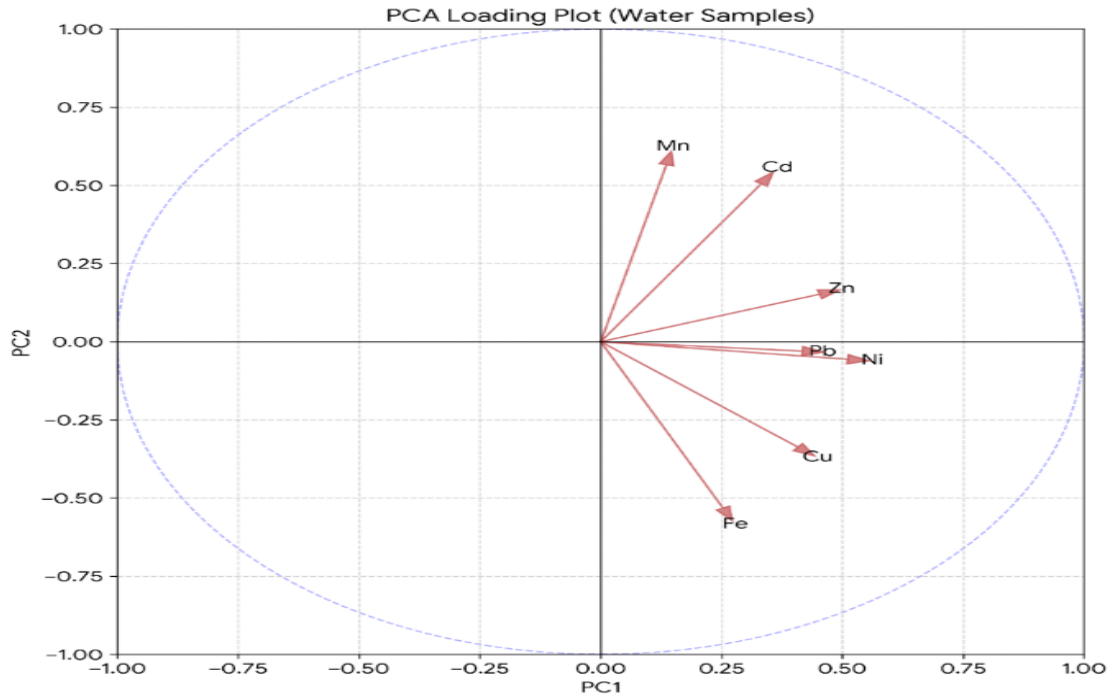


Figure 10: PCA biplot for water samples showing clustering patterns and potential source contributions of heavy metals

Table 8: Eigenvalues derived from PCA of sediment heavy metal concentrations showing dominant geochemical gradients.

| PC | Eigenvalue |
|-----|------------|
| PC1 | 3.029 |
| PC2 | 1.628 |
| PC3 | 1.431 |
| PC4 | 0.559 |
| PC5 | 0.316 |
| PC6 | 0.163 |
| PC7 | 0.074 |

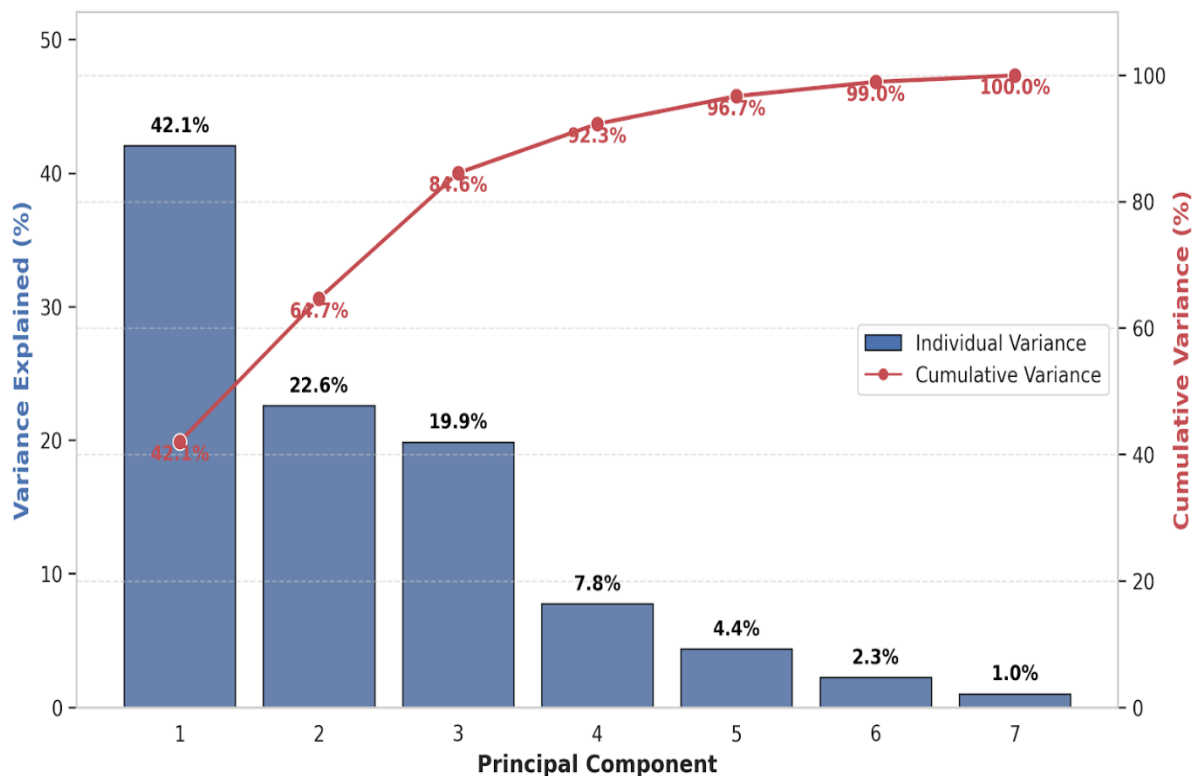


Figure 11: Scree plot showing eigenvalue distribution for sediment PCA.

Table 9: PCA loading matrix for sediment metals identifying underlying factors controlling sediment contamination patterns.

| Metal | PC1 | PC2 | PC3 | PC4 | PC5 | PC6 | PC7 |
|-------|--------|--------|--------|--------|--------|--------|--------|
| Pb | -0.144 | 0.742 | 0.022 | -0.017 | -0.014 | 0.650 | -0.074 |
| Cd | -0.356 | 0.456 | 0.318 | -0.419 | -0.062 | -0.610 | 0.114 |
| Mn | -0.430 | 0.012 | 0.321 | 0.668 | 0.460 | -0.116 | -0.203 |
| Fe | -0.079 | 0.317 | -0.692 | 0.449 | -0.301 | -0.340 | 0.080 |
| Cu | -0.506 | -0.233 | -0.225 | -0.253 | -0.241 | 0.069 | -0.716 |
| Zn | -0.417 | -0.130 | -0.464 | -0.294 | 0.574 | 0.122 | 0.405 |
| Ni | -0.482 | -0.265 | 0.223 | 0.165 | -0.554 | 0.238 | 0.508 |

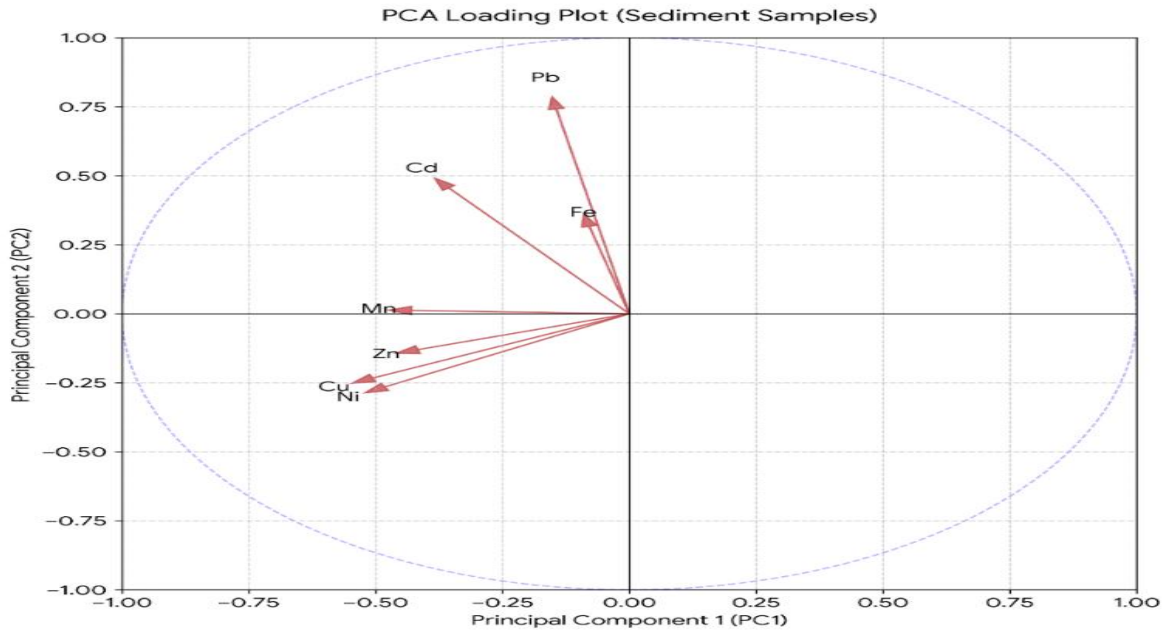


Figure 12: PCA biplot of sediment heavy metals illustrating dominant geochemical gradients and source associations.

Table 10: Mean-based sediment–water partition ratios showing distribution behaviour and affinity of heavy metals between aqueous and sedimentary phases.

| Metal | Mean Water | Mean Sediment | Partition Ratio (Sed/Water) |
|-------|------------|---------------|-----------------------------|
| Pb | 0.01778 | 0.55069 | 30.98 |
| Cd | 0.00279 | 0.06731 | 24.13 |
| Mn | 0.05097 | 13.71575 | 269.08 |
| Fe | 0.35665 | 537.39925 | 1506.81 |
| Cu | 0.09722 | 51.39314 | 528.62 |
| Zn | 0.14150 | 77.33278 | 546.52 |
| Ni | 0.04922 | 8.40719 | 170.80 |

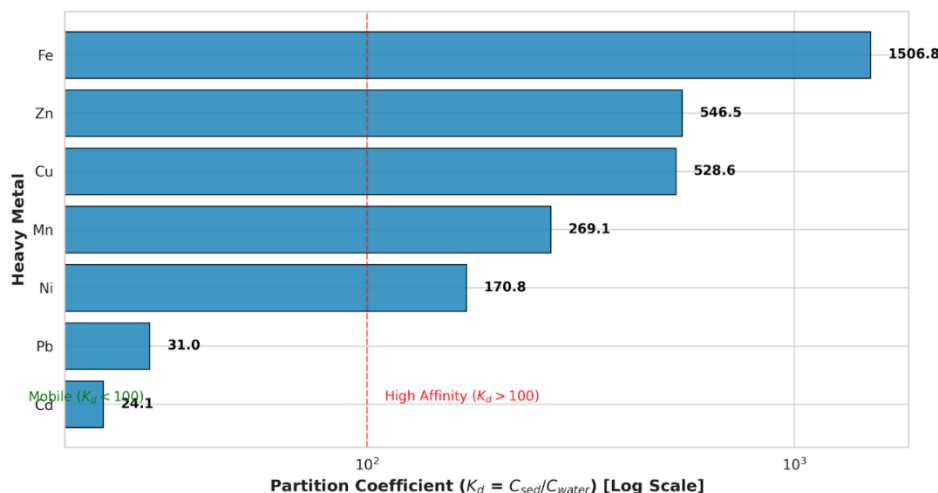


Figure 13: Sediment–water partitioning behaviour of heavy metals based on calculated partitioning coefficient.

CONCLUSION

This study demonstrates that heavy metal contamination in the Ikpoba and Ogba Rivers reflects the interaction between natural lithogenic processes and superimposed anthropogenic inputs associated with urbanization. Strong sediment enrichment and high sediment–water partition ratios indicate that sediments function as primary sinks controlling metal distribution, although redox-driven remobilization may pose future risks. Multivariate analysis confirms that Cd, Zn, Ni, Pb, and Cu are largely derived from common urban-industrial pathways, while Fe and Mn represent geogenic background influence. Although contamination indices suggest predominantly low to moderate pollution levels, elevated enrichment factors and the dominance of cadmium in ecological risk metrics highlight emerging environmental concern. The systems therefore represent transitional urban rivers experiencing cumulative stress rather than acute degradation. Effective management should prioritize controlling diffuse urban inputs, incorporating sediment monitoring into routine assessments, and evaluating bioavailability to better understand long-term ecological and human health implications.

REFERENCE

Abdu-Raheem, Oyebamiji, Afolagboye, & Talabi. (2024). Assessment of ecological and health risk impact of heavy metals contamination in stream sediments in Itapaji-Ekiti, SW Nigeria. *Journal of Trace Elements and Minerals*, 8, 100121. <https://doi.org/https://doi.org/10.1016/j.jtemin.2024.100121>

Adamu, Peter Godiya Nmagbo, Samson Likita Jawo, Onyeakazi Cynthia Chimobi, & Kunza. (2026).

Assessment of physicochemical properties of water and associated human health risk factors from Gitata river, Nasarawa state, Nigeria. *Journal of Basics and Applied Sciences Research*, 4(1), 113-119. <https://doi.org/10.4314/jobasr.v4i1.12>

Adeleke, Adegbite, Onifade, Sangoremi, & Adegbite. (2022). Seasonal variation of heavy metals concentration of industrial effluents and receiving rivers in Iguosa and Ikpoba, Benin City, Edo State, Nigeria. *Asian Journal of Applied Chemistry Research*, 11(1), 73-78.

Adubor, Ekperusi, Michael, & Olomukoro. (2025). Physicochemical Properties of Surface Water, Heavy Metals Levels in Sediments and Macrobenthic Invertebrates Community of Ikpoba River, Benin City, Edo State, Nigeria. *Journal of Applied Sciences and Environmental Management*, 29(5), 1653-1663.

Ali, Khan, & Ilahi. (2019). Environmental chemistry and ecotoxicology of hazardous heavy metals: environmental persistence, toxicity, and bioaccumulation. *Journal of chemistry*, 2019(1), 6730305.

Ansart, Quantin, Calmels, Allard, Roig, Coueffe, Heller, Pinna-Jamme, Nouet, Reguer, Vantelon, & Gautheron. (2022). (U-Th)/He Geochronology Constraints on Lateritic Duricrust Formation on the Guiana Shield. *Frontiers in Earth Science*,

Anyanwu. (2012). Physico-chemical and some trace metal analysis of Ogba River, Benin City, Nigeria. *Jordan Journal of Biological Sciences*, 147(617), 1-7.

Anyanwu, Davies, & Adetunji. (2023). Assessment of heavy metals in sediments and associated ecological risks in Ikwu River, Umuahia, Nigeria. *Assessment*, 8(3), 167.

- Ayedun. (2021). SEDIMENT QUALITY ASSESSMENT IN COASTAL COMMUNITIES OF ONDO STATE, NIGERIA. *Journal of Chemical Society of Nigeria*.
- Bawa-Allah. (2023). Assessment of heavy metal pollution in Nigerian surface freshwaters and sediment: A meta-analysis using ecological and human health risk indices. *Journal of Contaminant Hydrology*, 256, 104199.
- Chris, & Anyanwu. (2023). Assessment of some heavy metal content in sediments of a mangrove swamp, niger delta, nigeria using applicable ecological risk indices. *Acta Aquatica: Aquatic Sciences Journal*.
- Chris, Onyena, & Sam. (2023). Evaluation of human health and ecological risk of heavy metals in water, sediment and shellfishes in typical artisanal oil mining areas of Nigeria. *Environmental Science and Pollution Research*, 30, 80055-80069.
- Ekoa Bessa. (2023). Spatial Variation, Ecological Risk, and Point Sources of Environmental Trace Metals in Lacustrine Ecosystems: An Assessment of Natural and Urban Inputs. *Soil and Sediment Contamination: An International Journal*, 33, 1062 - 1086.
- Elarabi, Taha, & Elkhawad. (2013). Some Geological and Geotechnical Properties of Lateritic Soils from Muglad Basin Located in the South-Western Part of Sudan.
- Eyenubo, Ikpefan., Peretomode., F., Osakwe., & Awwioro. (2023). Accumulation and Risk Assessment of Heavy Metals in Sediments from Dredged Tributaries and Creeks of River Ethiop, South-South, Nigeria. *Journal of Physical Science*.
- Fadlillah, Utami, Rachmawati, Jayanto, & Widyastuti. (2023). Ecological risk and source identifications of heavy metals contamination in the water and surface sediments from anthropogenic impacts of urban river, Indonesia. *Heliyon*, 9(4).
- Ferrans, Jani, Burlakovs, Klavins, & Hogland. (2021). Chemical speciation of metals from marine sediments: Assessment of potential pollution risk while dredging, a case study in southern Sweden. *Chemosphere*, 263, 128105.
- Gampson, Dodd, & d'Entremont. (2025). Source and distribution of heavy metals in sediment samples from select creeks of the highly urbanized Metro Vancouver Watersheds, Canada. *Discover Environment*, 3.
- Hakanson. (1980). An ecological risk index for aquatic pollution control. A sedimentological approach. *Water research*, 14(8), 975-1001.
- Ibezute, Asibor, & Ibezute. (2016). Ecological assessment of brewery effluent impact on the macrobenthic invertebrates of Ikpoba River, Edo State, Nigeria. *International Journal of Ecosystem*, 6(3), 47-54.
- Imiuwa, Opute, & Ogbeibu. (2014). Heavy metal concentrations in Bottom Sediments of Ikpoba River, Edo State, Nigeria. *Journal of Applied Sciences & Environmental Management*, 18(1).
- Lynch, Batty, & Byrne. (2014). Environmental risk of metal mining contaminated river bank sediment at redox-transitional zones. *Minerals*, 4(1), 52-73.
- Maqsood, & Lobos-Moysa. (2025). Bottom Sediments as Dynamic Arenas for Anthropogenic Pollutants: Profiling Sources, Unraveling Fate Mechanisms, and Assessing Ecological Consequences. *International Journal of Molecular Sciences*, 26(20), 10219.
- Muller. (1969). Index of geoaccumulation in sediments of the Rhine River.
- Nkwunonwo, Odika, & Onyia. (2020). A review of the health implications of heavy metals in food chain in Nigeria. *The Scientific World Journal*, 2020(1), 6594109.
- Odo, Odo, & Odoabuchi. (2024). Evaluation of heavy metal pollution status of Anambra River basin using different indices: Examen de la contaminación por metales pesados de las aguas superficiales mediante índices de contaminación. *Sustainability, Agri, Food and Environmental Research-DISCONTINUED*, 12(2).
- Ogbeide, & Edene. (2023). Assessment of Physicochemical Properties of Water and Sediments in Ikpoba and Ogba Rivers, Edo State, Nigeria. *Journal of Applied Sciences & Environmental Management*, 27(6).
- Ogbeide, & Ogbeide. (2024). ARE OUR WATERS SAFE? INVESTIGATING HEAVY METAL RISKS IN THE IKPOBA RIVER ECOSYSTEM. *BIU Journal of Basic and Applied Sciences* 9(2), 198 – 215.,
- Ogbeide, & Okoduwa. (2024). Impact of Urban Runoff on Benthic and Pelagic Fish Fauna in Ikpoba River: Heavy Metals and Pathology of Liver Tissues. *NIPES-Journal of Science and Technology Research*, 6(2).
- Okafor, Omokpariola, Tabugbo, & Okoliko. (2024). Ecological and health risk assessments of heavy metals in surface water sediments from Ifite Ogwari community in Southeastern Nigeria. *Discover Environment*, 2.
- Okwodu, Okorie, & Nwoke. (2021). Determination and Evaluation of Heavy Metal Concentration in Surface

- Water and Sediment from Orashi River in Rivers State, Nigeria. *Current Journal of Applied Science and Technology*.
- Ologbosere, & Aluyi. (2016). Microbiological and physicochemical qualities of ikpoba river impacted by piped treated brewery effluent stream. *Nigerian Journal of Life Sciences (ISSN: 2276-7029)*, 6(1), 108-119.
- Prabakaran, Nagarajan, Eswaramoorthi, Anandkumar, & Franco. (2019). Environmental significance and geochemical speciation of trace elements in Lower Baram River sediments. *Chemosphere*, 219, 933-953.
- Qin, Enya, & Lin. (2018). Dynamics of Fe, Mn, and Al Liberated from Contaminated Soil by Low-Molecular-Weight Organic Acids and Their Effects on the Release of Soil-Borne Trace Elements. *Applied Sciences*.
- Sadiq, Usman Umar Kunji, & Vahyala I.E. (2026). Assessment of sediment yield using the erosion potential method (epm) in Yola South North-Eastern Nigeria. *Journal of Basics and Applied Sciences Research*, 4(1), 120-130. <https://doi.org/10.4314/jobasr.v4i1.13>
- Sani, Idris, Abdullahi, & Darma. (2022). Bioaccumulation and health risks of some heavy metals in *Oreochromis niloticus*, sediment and water of Challawa river, Kano, Northwestern Nigeria. *Environmental Advances*, 7, 100172. <https://doi.org/https://doi.org/10.1016/j.envadv.2022.100172>
- Shinkafi, Mubarak, & Abdulhamid. (2023). Analysis of Heavy Metals Contaminating Water and Fish Species in Kwanar-Are Dam, Katsina State, Nigeria. *UMYU Scientifica*, 2(4), 130-135.
- Swanson, Langman, Child, Wilhelm, & Moberly. (2023). Iron and manganese oxidation states, bonding environments, and mobility in the mining-impacted sediments of coeur d' alene lake, idaho: Core experiments. *Hydrology*, 10(1), 23.
- Tiabou, Takem-Agbor, Yiika, Eseyu Mengu, Kachoueiyan, & Agyingi. (2024). Distribution, source apportionment and ecological risk assessment of heavy metals in Limbe River sediments, Atlantic Coast, Cameroon Volcanic Line. *Discover Water*, 4(1), 62.
- Tomlinson, Wilson, Harris, & Jeffrey. (1980). Problems in the assessment of heavy-metal levels in estuaries and the formation of a pollution index. *Helgoländer meeresuntersuchungen*, 33(1), 566-575.
- Uwaifo, Egun, & Agho. (2023). Ecotoxicological risk assessment of metalloids contamination in the sediment and benthic fauna of a tropical lotic freshwater ecosystem in Southern Nigeria. *Biologija*.
- Wangboje, & Braimah. (2022). ASSESSMENT OF HEAVY METAL CONTAMINATION IN WATER AND SELECTED PISCICAN BIO-INDICATORS FROM OGBA RIVER BENIN CITY NIGERIA. *Journal of Engineering for Development*, 14(1), 46-62
- Wangboje, & Ekundayo. (2013). Assessment of heavy metals in surface water of the Ikpoba reservoir, Benin City, Nigeria. *Nigerian Journal of Technology*, 32(1), 61-66.